Macromolecules
ARTICLE
pubs.acs.org/Macromolecules

How Fast Can a CRP Be Conducted with Preserved Chain End Functionality?

Mingjiang Zhong and Krzysztof Matyjaszewski*

Center for Macromolecular Engineering, Department of Chemistry, Carnegie Mellon University, 4400 Fifth Avenue, Pittsburgh, Pennsylvania 15213, United States

S Supporting Information

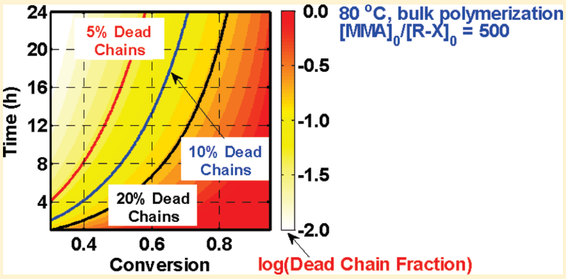

ABSTRACT: The preservation of chain end functionality (CEF) is perhaps the most important criterion of the "livingness" for any controlled/living radical polymerization (CRP) system. CEF depends on several parameters but most importantly on concentration of propagating radicals, i.e., rate of polymerization. There are claims in the literature about ultrafast CRP leading to ultrahigh molecular weight with perfectly preserved CEF. However, faster CRP always results in lower CEF. Thus, how fast can a CRP be conducted with preserved CEF? In this paper we evaluate, by kinetic analysis and computation, the dependence of CEF on the rate of polymerization, monomer structure (rate constants of propagation and termination), targeted degree of polymerization, initial monomer concentration, and monomer conversion. Some subtle differences in the definition of CEF are discussed for different types of atom transfer radical polymerization (ATRP) techniques. CEF for polymer chains with and without an α-alkyl group from a (macro)initiator are compared for a normal ATRP and initiators for continuous activator regeneration (ICAR) ATRP. The latter system closely resembles reversible addition−fragmentation transfer (RAFT) polymerization.

INTRODUCTION

Since living anionic polymerization was discovered in 1956,[1,2] a variety of controlled/living polymerization methods have been developed to prepare well-defined (co)polymers.[3−9] The development of controlled/living polymerization opened new ways to precisely design polymers with complex architecture.[10−12] Recently, controlled/living radical polymerization (CRP) has evolved into one of the most powerful controlled/living polymerization methods and attracted increasing levels of attention in different areas of chemistry and materials science.[5] CRP has been successfully used to synthesize polymers with controlled molecular weight (MW), molecular weight distribution (MWD), topology, composition, and functionality.

Three fundamental CRP systems (Scheme 1) have attracted the most attention: stable free radical polymerization (SFRP),[13,14] atom transfer radical polymerization (ATRP),[15−21] and degenerative chain transfer polymerization (DT).[22−26] In these procedures control is achieved through a dynamic equilibration between a predominant fraction of dormant species and a low concentration of propagating radicals.[27−30]

SFRP utilizes stable free radicals ($X^\bullet$) which neither directly react with monomer nor itself, but only act as reversible trapping agents for the propagating radical.[13,14] ATRP employs a reversible transition metal mediated catalytic redox process. The dormant species is activated by a lower oxidation state metal catalyst complex; copper-based catalysts are most often used to generate a propagating radical and a higher oxidation state metal complex which serves as a deactivator. Several other initiation/activation systems were developed in addition to the originally developed "normal" initiation system for an ATRP (normal ATRP), where the lower oxidation state transition metal complex is added to the reaction. Among these techniques, reverse ATRP,[31] simultaneous reverse and normal initiation (SR&NI),[32]

Scheme 1. Three Typical CRP Systems

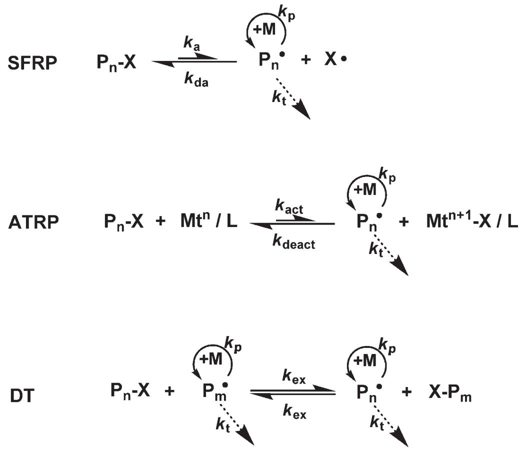

Received: December 13, 2010
Revised: February 5, 2011
Published: March 22, 2011

dx.doi.org/10.1021/ma102834s | *Macromolecules* 2011, 44, 2668–2677

and activator generated by electron transfer (AGET)[33] systems were developed to overcome problems associated with fortuitous oxidation of active catalyst complexes. Two activator regeneration procedures were developed to diminish the amount of catalyst used in the reaction: activator regenerated by electron transfer (ARGET)[34] and initiators for continuous activator regeneration (ICAR).[35]

Both SFRP and ATRP follow kinetic patterns consistent with the persistent radical effect (PRE).[36−38] This contrasts with polymerizations involving DT process, which are not based on the PRE. Reversible addition−fragmentation chain transfer (RAFT) polymerization[22] which is the most often used DT system achieves control by a fast exchange among active and dormant species using an efficient degenerative chain transfer agent (CTA). It requires continuous source of additional initiating radicals, normally provided by slow decomposition of a free radical initiator, to compensate for unavoidable termination reactions.

Independent of the mechanism of exchange between active and dormant species, propagation and termination steps are the same in any radical polymerization. Therefore, the rate of propagation (R_p) is proportional to the propagation rate constant (k_p), the concentrations of monomer ([M]) and propagating radical ($[R^\bullet]$) as expressed in eq 1, where t is polymerization time.

$$R_p = -\frac{d[M]}{dt} = k_p[M][R^\bullet] \tag{1}$$

According to eq 1, for the same monomer, faster polymerization requires higher $[R^\bullet]$. However, increased radical concentration results in faster bimolecular termination. Equation 2 describes how fast dead chains are generated through disproportionation termination.

$$R_t = \frac{d[T]}{dt} = 2k_t[R^\bullet]^2 \tag{2}$$

where k_t is the termination rate constant and [T] is the concentration of the dead chains caused by termination. To describe general systems with the coexistence of termination by disproportionation and combination, [T] should be defined as the concentration of lost living chains. It is also assumed that the formation of dead chains by other mechanisms can be neglected. Thus, the penalty for faster polymerization (i.e., higher radical concentration) is progressively higher proportion of terminated chains and loss of livingness. The fraction of extendable chains is referred as chain end functionality (CEF). Consequently, for any CRP to preserve a specific value for CEF, a minimal time is required. Nevertheless, there are frequent claims in the literature about very fast CRP with preserved functionality.[39,40] However, faster CRP must lead to lower CEF. As will be shown later, this time primarily depends on the type of monomer (propagation rate constant and termination rate constant), targeted degree of polymerization (DP_T), initial monomer concentration, and targeted monomer conversion.

Well-defined functional polymers made by CRP require high CEF.[41] Retention of CEF is needed for synthesis of various telechelic polymers used in postpolymerization reactions, segmented copolymers, and especially block copolymers. Linear living polymers starting from original living chain initiator or CTA R-X should result in the formation of a polymer with R-$(A)_n$-X structure, when polymerizing monomer A. The telechelic polymer can be extended by monomer B to form a block copolymer R-$(A)_n$-*b*-$(B)_n$-X, if the X functionality at the chain end is preserved. For most CRP techniques including NMP, normal ATRP, and ARGET ATRP, the concentration of chains carrying X group decreases due to termination reactions, and there are two chains populations: R-$(A)_n$-X and R-$(A)_n$ (in addition to ppm amounts growing radical R-$(A)_n^\bullet$). However, in RAFT polymerization and ICAR ATRP systems, concentration of chains with X group is essentially constant, although their fraction decreases due to terminated chains and new chains generated from extra radical inititors ($I^\bullet$). Thus, there are four chain populations: R-$(A)_n$-X, R-$(A)_n$, I-$(A)_n$-X and I-$(A)_n$. Consequently, CEF should be specifically defined in these systems since I-$(A)_n$-X could be considered as a type of extandable chain which lost the initial α-CEF. This type of chain formed during chain extension targeting a block copolymer will consist of the second homopolymer. A kinetic simulation of an ICAR ATRP will be presented in order to distinguish these two types of CEFs.

COMPUTER SIMULATIONS

Predici, version 6.3.2, was used for all kinetic modeling, as all other previous simulations.[42−47] An adaptive Rothe method is employed in Predici as a numerical strategy for time discretization.[48] The number-average degree of polymerization (DP) and MWD (M_w/M_n) were calculated for all the polymers, including the dormant species, propagating species, and terminated chains. Kinetic models and rate constants for ICAR ATRP and normal ATRP are provided in the Supporting Information.

RESULTS AND DISCUSSION

Derivation of Dead Chain Fraction (DCF) Equation for CRP. In the following derivations, it is assumed that $[R^\bullet]$ does not change during polymerization. In many CRP systems, linear first-order kinetic plots are observed, indicating constant radical concentration, due to either steady state by equal rates of initiation and termination (DT systems) or balanced activation and deactivation and negligible termination for PRE systems. This should be valid at least for reactions where a relatively small fraction of chains are lost by termination. At constant $[R^\bullet]$, the integration of eq 1 gives the relationship among polymerization time (t), monomer conversion (p) and $[R^\bullet]$.

$$\ln(1-p) = -k_p[R^\bullet]t \tag{3}$$

The concentration of terminated chains can be calculated by the integration of eq 2.

$$[T] = 2k_t[R^\bullet]^2 t \tag{4}$$

The combination of eq 3 and eq 4 yields the concentration of terminated chains as a function of time and conversion.

$$[T] = \frac{2k_t[\ln(1-p)]^2}{k_p{}^2 t} \tag{5}$$

The DP_T is defined by the ratio between initial monomer concentration, $[M]_0$, and the concentration of living polymers, [P−X], which is equal to initiator concentration, $[R-X]_0$, for the quantitative initiation. Hence, the dead chains fraction (DCF) can be expressed as eq 6.

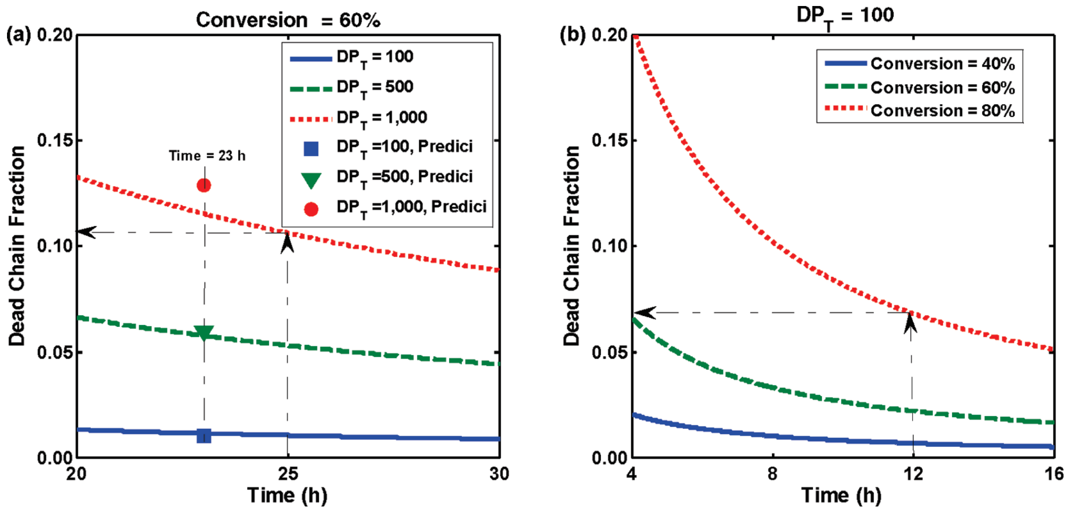

Figure 1. Plots of DCF vs polymerization time for bulk polymerization of MMA at 80 °C. (a) Three different DP$_T$s and aiming at 60% conversion. (b) Aiming different conversions for DP$_T$ = 100.

$$\mathrm{DCF} = \frac{[\mathrm{T}]}{[\mathrm{R-X}]_0} = \frac{2\mathrm{DP_T}k_t[\ln(1-p)]^2}{[\mathrm{M}]_0{k_p}^2t} \tag{6}$$

To simplify calculations, we neglected the decrease in the number of chains by bimolecular combination (corresponding to quantitative disproportionation). However, the same conclusions are qualitatively valid for systems with combination. Thus, the DCF defines the fraction of living chains lost from the initial living chains. Knowing DCF, one can calculate the CEF by eq 7.

$$\mathrm{CEF} = 1 - \mathrm{DCF} \tag{7}$$

Equation 6 suggests that there are several strategies that can be employed to decrease the fraction of dead chains: slowing down the rate of polymerization (larger t), quenching the reaction at lower monomer conversion (smaller p), targeting lower DP$_T$, using higher initial monomer concentration (larger $[\mathrm{M}]_0$) or choosing monomers with an inherently lower value of $k_t/(k_p)^2$. In the following discussion, we will discuss in detail every parameter which is involved in eq 6 and determine how they influence CEF.

Minimizing Polymerization Time for a CRP. Since eq 6 includes six parameters, a straightforward way to conduct the evaluation is to fix some of the parameters and analyze how the remaining one or two parameters affect the DCF. To simplified the system, we first present results with rate constants independent of polymer chain length. For example, for the bulk polymerization of methyl methacrylate (MMA) at 80 °C: k_t (9.00×10^7 M^{-1} s^{-1}), k_p (1300 M^{-1} s^{-1}), and $[\mathrm{M}]_0$ (9.34 M) are constants and one can clearly observe the effect of polymerization time, monomer conversion, and DP$_T$ on DCF.

How fast a polymerization can be conducted is one of the most important questions in all types of polymerizations, since it allows one to complete a particular synthetic task quicker. In a CRP a low concentration of propagating radicals is required to minimize termination reactions and achieve a controlled process. As expressed in eq 1, polymerization time is determined by $[\mathrm{R}^\bullet]$. The correlation between CEF and rate of polymerization is defined by $[\mathrm{R}^\bullet]$. If k_t, k_p, and $[\mathrm{M}]_0$ are fixed, based on the conditions defined above, then eq 6 shows that DCF is inversely proportional to polymerization time when targeting a certain DP$_T$ and a specific degree of conversion (eq 8).

$$\mathrm{DCF} = C_1t^{-1}, \quad C_1 = \frac{2\mathrm{DP_T}k_t[\ln(1-p)]^2}{[\mathrm{M}]_0{k_p}^2} \tag{8}$$

In eq 8, C_1 is a constant when every parameter except t is fixed. Figure 1 illustrates the relationship of DCF and the rate of polymerization in two ways. In Figure 1a three different DP$_T$s are targeted at 60% conversion, while Figure 1b is focused on targeted DP$_T$ = 500 but at different degrees of conversions. Both procedures show a similar trend that a reduced fraction of dead chains, or increased livingness, can be achieved by slowing down the polymerization. Both higher DP$_T$ and higher conversion give larger value for C_1, according to eq 8. However, curves with higher DP$_T$ or higher conversion give steeper slope than the lower values. For example, in Figure 1a the DCF decreased with polymerization time, and this decrease was more dramatic when DP$_T$ = 1000 than the other two cases targeting lower DP$_T$s. Therefore, slowing down the CRP can increase CEF, and this becomes more significant at higher conversion or in higher DP$_T$ systems. Inspection of Figure 1 shows that targeting DP$_T$ = 1000 at 60% conversion in 25 h leads to 11% of dead chains (CEF = 89%). In addition, for DP$_T$ = 100 and conversion 80%, reaction performed within 12 h leads to 7% of dead chains.

In many CRPs straight semilogarithmic kinetic plots imply essentially constant $[\mathrm{R}^\bullet]$. Therefore, eq 6 was derived assuming constant $[\mathrm{R}^\bullet]$ although this may not be always correct. To evaluate potential error, a series of Predici simulations were conducted to compare with the values predicted from eq 6, as shown in Figure 1a. In these simulations, normal ATRP systems target DP$_T$ = 100, 500, and 1000 and reach 60% conversion in 23 h (detailed conditions and models are provided in the Supporting Information). The value of DCF for DP$_T$ = 1000 calculated based on eq 6 is 10% smaller than obtained from Predici simulation. For DP = 500 it is 3% smaller, and it is essentially the same for DP$_T$ = 100. This could be attributed to the larger decrease of $[\mathrm{R}^\bullet]$ for the DP$_T$ = 1000 system. Since the error of DCF calculated from eq 6 should increase with proportion of terminated chains, we subsequently analyzed systems with DCF not exceeding 20%.

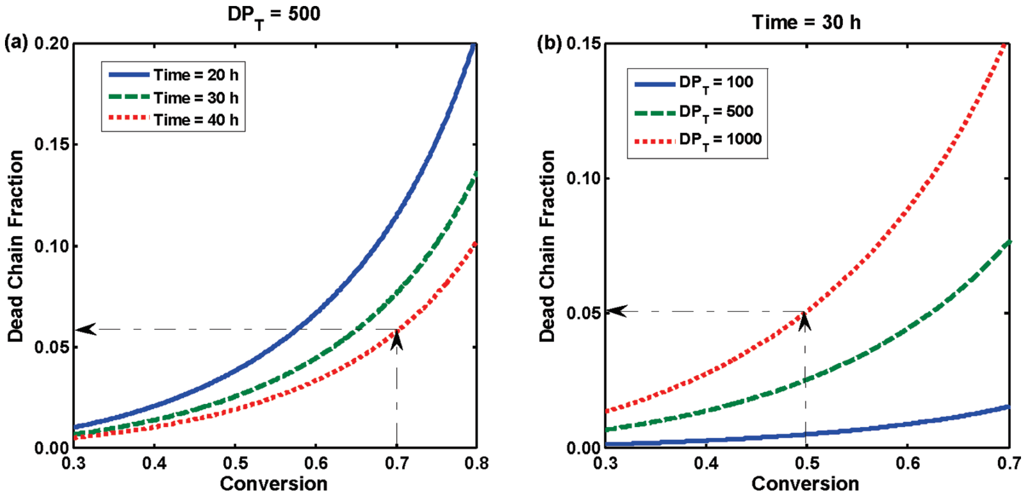

Figure 2. Plots of DCF vs conversion for bulk polymerization of MMA at 80 °C. (a) Three different rates of polymerization for $\mathrm{DP_T}$ = 500. (b) Achieving three different conversions in 30 h.

A simple transformation of eq 8 provides another expression for factors influencing CEF

$$t = C_1 \frac{1}{\mathrm{DCF}}, \quad C_1 = \frac{2\mathrm{DP_T}k_t[\ln(1-p)]^2}{[\mathrm{M}]_0 k_p^{\,2}} \qquad (9)$$

Equation 9 shows that under certain CRP conditions a specific DCF corresponds to a specific rate of polymerization. In other words, if there is a lower limit to the DCF which can be tolerated, the calculated value for t via eq 9 indicates how much time should be spent on the polymerization. For a given condition, constant C_1, the required minimal polymerization time, can be predicted according to the acceptable DCF. In order to achieve this minimal time in a specific CRP technique, the conditions require a specific maximal $[\mathrm{R}^\bullet]$. This $[\mathrm{R}^\bullet]$ value can be attained by properly tuning specific reaction conditions in any CRP technique, such as the ratio of $\mathrm{Cu^{II}}$ to $\mathrm{Cu^{I}}$ species in a normal ATRP, the rate of feeding the extra initiator in a RAFT polymerization and in an ICAR ATRP, the rate of the reduction process in ARGET ATRP, etc.[5]

Influence of Conversion on DCF. Another question is how DCF is affected by conversions. Equation 10, another form for eq 6, answers this question.

$$\mathrm{DCF} = C_2[\ln(1-p)]^2, \quad C_2 = \frac{2\mathrm{DP_T}k_t}{[\mathrm{M}]_0 k_p^{\,2} t} \qquad (10)$$

Equation 10 reveals that a polymerization targeting a certain $\mathrm{DP_T}$ will lose more living chains when achieving higher conversion within the same time. This results from the fact that a higher $[\mathrm{R}^\bullet]$ is required to complete the polymerization in the targeted time. Figure 2 illustrates this in two ways, using an example of MMA bulk polymerization at 80 °C. C_2 in eq 10 increases with $\mathrm{DP_T}$ but decreases with polymerization time. Figure 2 shows that the DCF increases faster with conversion in the case of shorter polymerization time and higher $\mathrm{DP_T}$. According to Figure 2, targeting 70% conversion in 40 h leads to 6% of dead chains for $\mathrm{DP_T}$ = 500. For $\mathrm{DP_T}$ = 1000 with 30 h targeted polymerization time, reaction only loses 5% of living chains to achieve 50% conversion.

Influence of $\mathrm{DP_T}$ on DCF. In the discussion about polymerization rate and conversion, we noticed that $\mathrm{DP_T}$ is also an important factor for DCF. To reach the same conversion with the same preservation of CEF in higher $\mathrm{DP_T}$ systems, the rate of polymerization should be decreased. Equation 11 gives a linear relationship between DCF and $\mathrm{DP_T}$. The relationship for bulk polymerization of MMA at 80 °C is illustrated in Figure 3. The linear slopes decrease with polymerization time but increase with conversion. Figure 3a shows that 89% CEF can be preserved when targeting $\mathrm{DP_T}$ = 800 and achieving 60% conversion within 20 h. Reaching 80% conversion within 30 h results in 16% of dead chains when targeting $\mathrm{DP_T}$ = 600.

$$\mathrm{DCF} = C_3\mathrm{DP_T}, \quad C_3 = \frac{2k_t[\ln(1-p)]^2}{[\mathrm{M}]_0 k_p^{\,2} t} \qquad (11)$$

Preparation of a Polymer with a Specific DP. It is possible to prepare a polymer with a specific DP by changing more than one parameter. For instance, the same DP can be reached by targeting higher $\mathrm{DP_T}$ at lower conversion or targeting lower $\mathrm{DP_T}$ at higher conversion. Which approach provides lower DCF within the same time? Both higher $\mathrm{DP_T}$ and higher conversion lead to more dead chains at the same polymerization rate. Since DP can be expressed as the product of $\mathrm{DP_T}$ and conversion, i.e., DP = $\mathrm{DP_T} \times p$, eq 6 converts to

$$\mathrm{DCF} = \frac{2\mathrm{DP}k_t}{[\mathrm{M}]_0 k_p^{\,2} t} \frac{[\ln(1-p)]^2}{p} \qquad (12)$$

In eq 12, the second term of the product $([\ln(1-p)]^2/p)$ is an increasing function of p. Since the first term in the equation contains two rate constants and three fixed values, it remains constant and DCF increases with p. Hence, the combination of higher $\mathrm{DP_T}$ and lower conversion gives less dead chains when targeting a certain polymer DP within the same polymerization time.

Figure 4 shows an example of the DCF formed during formation of PMMA with different DPs. In this plot, every point on the 3D surface stands for one polymerization reaction terminated within 5 h. In the same curve the product of conversion and $\mathrm{DP_T}$ is a fixed value. Along the same curve, the desired DP does not change, while the trend of DCF obeys the above conclusion. For instance, if one wants to synthesize PMMA with DP = 60, one could target $\mathrm{DP_T}$ = 75, 100, and 150 but stop the reaction at 80%, 60%, and 40% conversion, respectively. On the

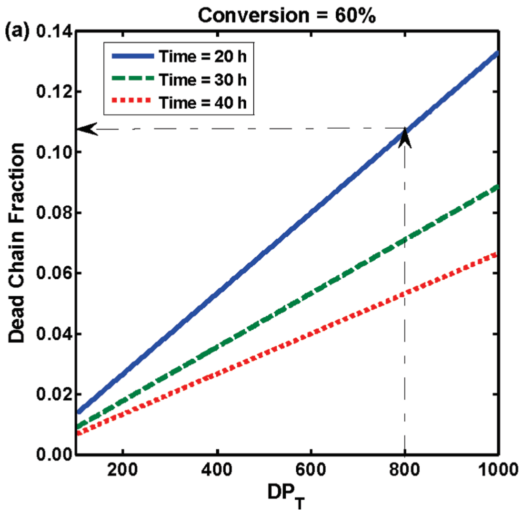

Figure 3. Plots of DCF vs DP_T for bulk polymerization of MMA at 80 °C. (a) Three different rates of polymerization at 60% targeted conversion. (b) Three different conversions reached in 30 h.

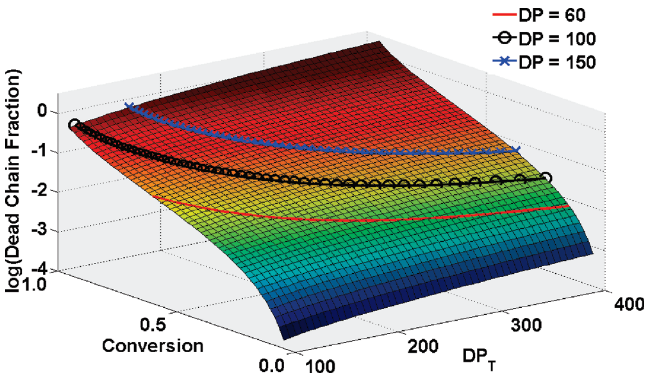

Figure 4. Plot of logarithmic value of DCF vs conversion and DP_T for PMMA for three different desired DPs. Conditions: 80 °C; bulk polymerization, 5 h.

basis of the data in Figure 4, those three systems will generate polymers with DCF = 12.3%, 5.3%, and 2.5%, respectively. Thus, synthesis of DP_T = 150 at 40% conversion gives 5 times lower DCF than aiming at DP_T = 75 at 80% conversion in preparation of PMMA with DP = 60!

Influence of Initial Monomer Concentration on DCF. Previous example showed that polymerization diluted by monomer is better controlled. Can dilution by solvent also provide better control? The addition of a solvent may be sometimes necessary to improve the solubility of the polymer or catalyst or to control the viscosity of the system. The role of solvent is not the same as that of monomer, and eq 13 shows that solvent is not a good diluent for decreasing DCF because it actually reduces $[M]_0$ correspondingly increasing DCF.

$$\mathrm{DCF} = \frac{C_4}{[\mathrm{M}]_0}, \quad C_4 = \frac{2\mathrm{DP_T}k_t[\ln(1-p)]^2}{{k_p}^2 t} \qquad (13)$$

In comparison with bulk polymerization, when monomer is diluted by solvent, the radical concentration must increase in order to maintain the same polymerization rate. This causes more termination at the same rate of polymerization. Figure 5 shows the DCF after 10 h for a MMA polymerization conducted at 80 °C targeting DP_T = 100. At the same conversion, bulk polymerization always gives a lower DCF. Selecting the point at 70% conversion from each of these three curves, bulk polymerization generates only 4.6% of dead chains while the other two DCFs are 6.9% and 9.2%, respectively.

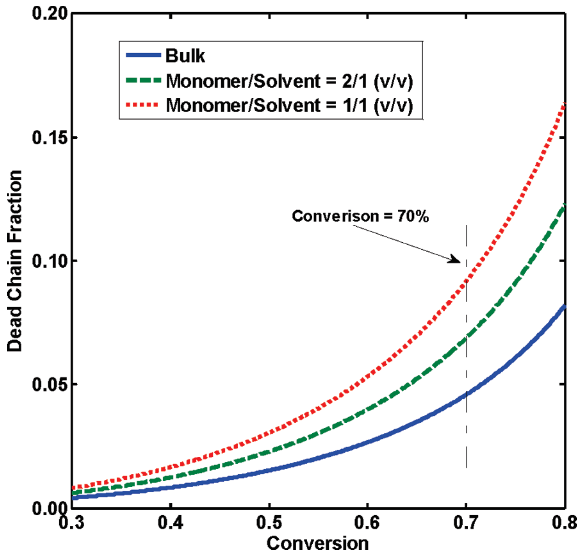

Figure 5. Comparison of DCFs for three systems with different initial monomer concentrations. Conditions: 80 °C, $[MMA]_0/[R\text{-}X]_0$ = 100/1, 10 h.

Effect of k_t and k_p Values on DCF and Minimal Polymerization Time. Results presented above are universal for any CRP. Higher CEF requires slower polymerization, higher monomer concentration, lower DP_T, and stopping the polymerization at lower conversion. However, the relationship between "how fast" and "how living" a CRP is strongly depends on the polymerized monomers and more specifically on k_p and k_t values. Equation 14 shows that lower $k_t/(k_p)^2$ value gives less dead chains under certain condition (constant C_5), thus low k_t and high k_p are both desired.

$$\mathrm{DCF} = C_5\frac{k_t}{{k_p}^2}, \quad C_5 = \frac{2\mathrm{DP_T}[\ln(1-p)]^2}{[\mathrm{M}]_0 t} \qquad (14)$$

Table 1. Minimal Time for the Polymerization of MA, MMA, and St with CEF = 90%[a]

			$DP_T = 500$		$DP_T = 100$	
monomer	k_p $(M^{-1}\,s^{-1})^b$	k_t $(M^{-1}\,s^{-1})^b$	$p = 60\%$	$p = 90\%$	$p = 60\%$	$p = 90\%$
MA	13 200	1.10×10^8	*8.0 min*	**50.6 min**	1.6 min	**10.1 min**
MMA	1300	9.00×10^7	*13.3 h*	83.9 h	2.7 h	16.8 h
St	665	1.10×10^8	*2.8 days*	17.5 days	***0.6 days***	***3.5 days***

[a] Conditions: 25 °C,(MA) and 80 °C (MMA and St), $[M]_0/[R\text{-}X]_0 = DP_T/1$, bulk polymerization. [b] k_p and k_t values were obtained or estimated from literature.[49−53] k_t value is the sum of k_{tc} (the combination rate constant) and k_{td} (the disproportionation rate constant).

In radical polymerization, termination is often a diffusion-controlled process, and the difference between termination rate constants for different monomers is small. However, propagation rate constants depend strongly on monomer structure. For example, at 80 °C, the k_p of styrene (St) is ca. 2 times smaller than that of MMA but nearly 2 orders of magnitude smaller than that of methyl acrylate (MA). Table 1 gives corresponding rate constants and values for 90% preservation of CEF for these three monomers. Values in Table 1 for MMA and St correspond to 80 °C but for MA to 25 °C. Minimal time values, calculated for MA polymerization at 80 °C are lower than those at 25 °C, and are equal to 37 sec, 234 sec, 7 sec, 48 sec, correspondingly. Three "contour maps" are plotted in Figure 6 for the bulk polymerization of MA, MMA, and St targeting the same $DP_T = 500$. Each contour corresponds to the logarithmic value of DCF, and three solid lines show the relationship between reaction time and conversion for DCF = 5%, 10%, and 30%. For example, it is possible to prepare poly(methyl acrylate) (PMA) with 90% preserved CEF for $DP_T = 500$ and reaching 90% conversion in 8 min! However, as highlighted by italicized entries in Table 1, the same control requires 13 h for PMMA and 2.8 days for polystyrene (PSt)! Bold entries show the effect of DP_T for 500 and 100 values for PMA at 90% conversion. The former requires 50 min but the latter only 10 min. Finally, bold-italicized entries show that the same CEF = 90% for PSt and $DP_T = 100$ requires 3.5 days at 90% but only 0.6 days at 60% conversion.

Evaluation by Chain Length Dependent Termination (CLDT). The "maps" above were constructed for constant values of termination rate coefficients. However, since termination is diffusion limited, it strongly depends on viscosity and chain length. Thus, the CLDT rate coefficients strongly depend on both conversion and DP.[53] The effect of CLDT rate coefficient was analyzed as a function of DP and conversion for bulk polymerization of MMA and MA at 80 °C.[54,55] Figure 7 provides a more accurate evaluation of DCF of PMMA by integrating the CLDT data. Detailed information on how to calculate DCF based on CLDT is provided in the Supporting Information. The system with $DP_T = 500$ (Figure 7a) does not show a significant difference compared to the non-CLDT evaluation. However, in the $DP_T = 5000$ system (Figure 7b), the curves for specific DCFs display a dramatic drop in termination reactions, which means that much faster polymerization can be conducted for system with a high DP_T. For example, to preserve 90% CEF at 50% conversion targeting PMMA with $DP_T = 5000$, it requires 40 h, which is nearly 2 times faster than that predicted by non-CLDT.

Although the required rate of polymerization for acceptable CEF depends on the type of monomer, there are some other possibilities to decrease $k_t/(k_p)^2$ via tuning various reaction conditions. For example, an increase of temperature results in an increase in the polymerization rate without a significant loss of CEF since higher temperatures increases k_p much more than k_t due to lower activation energy of termination compared to that of propagation. However, there is a limit in temperature increase due to chain transfer (e.g., acrylates), self-initiation (e.g., St), depropagation (e.g., methacrylates), and other side reactions involving the mediating agent (e.g., disproportionation in NMP). Pressure is another important parameter.[56] Radical propagation has a negative volume of activation while termination has a positive one, and higher pressure not only enhances k_p but also reduces k_t. This strategy has been successfully applied to synthesize high MW polymers by AGET ATRP[57] and RAFT polymerization.[58−61]

CEF in CRP Systems Involving Extra Radical Initiators. There are several CRP processes relying on the DT mechanism, such as RAFT polymerization, that employs radical initiators (e.g., azobis(isobutyronitrile) (AIBN)). To this category also belongs ICAR ATRP. As mentioned in the Introduction, the radical initiators continuously generate new chains. Thus, there are two populations of living chains: those generated from the original (macro)initiator R-X and newly generated, also extendable chains I-X and I-P-X. The R group may play an important role. It can be the first block in a block copolymer, and it can represent a surface in surface-initiated CRP or a specific functionality in telechelics. Thus, although I-X and I-P-X species can grow, they will not contain an important R moiety. Therefore, it is useful to define two types of CEF in the systems involving radical initiators. The first definition is similar to the general case for CRP, which is the fraction of all extendable chains (P-X), and the second one describes the fraction of chains with dual functionality (R-P-X). Since extendable species include initiator and living polymer, to simplify the following discussion, we define [R-P-X] as the total concentration of dual functionalized chains including R-P-X chains and original initiator R-X. Similarly, [I-P-X] contains I-P-X chains and newly generated initiator I-X. Thus, [P-X] is the sum of [R-P-X] and [I-P-X].

In RAFT and other DT polymerizations a steady state exists between the rate of decomposition of the added radical initiator and termination processes (eqs 2, 15, and 16). Thus, $[R^\bullet]$ is determined in eq 17, as in a standard free radical polymerization (FRP).

$$R_i = R_t \tag{15}$$

$$R_i = 2k_{dc}f[I_2] \tag{16}$$

$$[R^\bullet] = \sqrt{\frac{k_{dc}f[I_2]}{k_t}} \tag{17}$$

ICAR ATRP (Scheme 2) also follows the same kinetics.[35] In the following discussion, CEF in ICAR ATRP is analyzed using different criteria. Since ICAR ATRP and other DT processes (as RAFT polymerization) follow similar kinetics, the results will provide more general conclusions for all DT systems. According to eq 17, ICAR ATRP is accelerated in the presence of large concentration of radical initiators. However, although such systems, also named as hybrid ATRP,[40] result in faster polymerization, they also result in a larger loss of CEF. The number of polymer chains with dual α-ω-functionality drops significantly with increased radical initiator concentration. In order to define the fraction of two types of CEF formed in these systems, a series of simulations were carried out for ICAR ATRP. In these

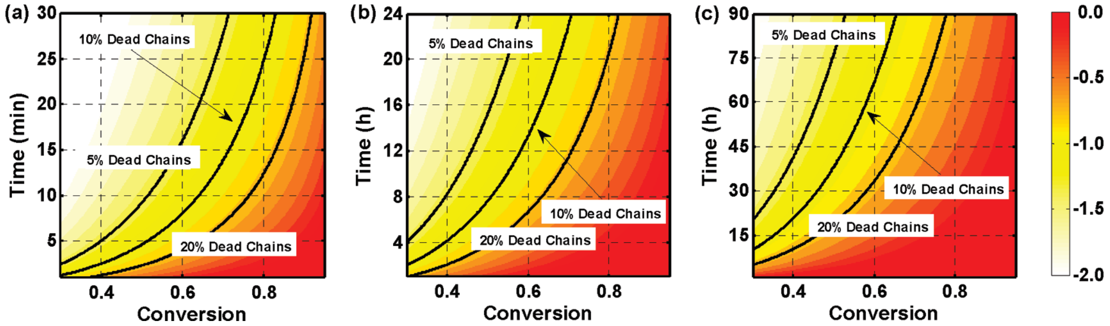

Figure 6. Contour maps for DCF as a function of conversion and polymerization time for different monomers: (a) MA, (b) MMA, and (c) St. Conditions: 25 °C (MA) and 80 °C (MMA and St), $[M]_0/[R\text{-}X]_0 = 500/1$, bulk polymerization. Scale bar represents the logarithmic value of DCF for (a), (b), and (c).

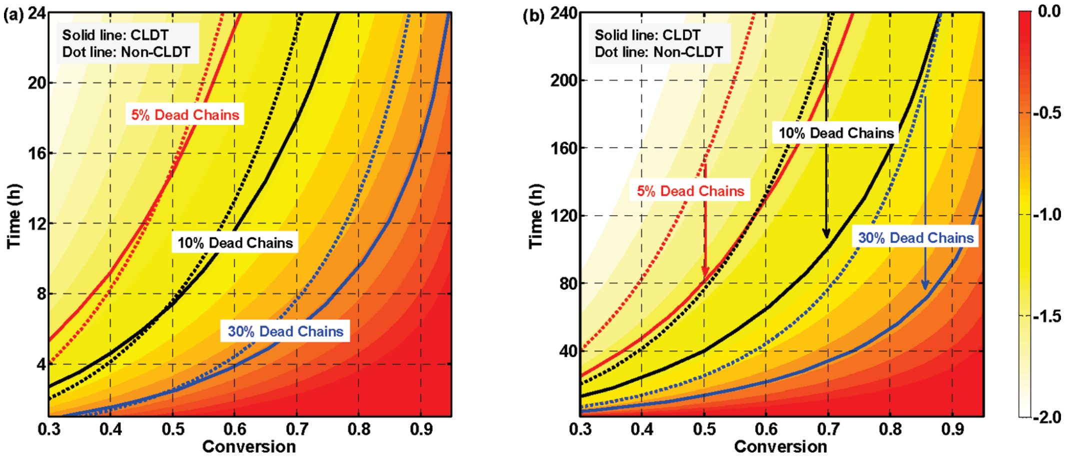

Figure 7. Plots comparing DCF of PMMA computed with and without CLDT. (a) $DP_T = 500$; (b) $DP_T = 5000$. Conditions: 80 °C, $[M]_0/[R\text{-}X]_0 = 500/1$, bulk polymerization. Scale bar represents the logarithmic value of DCF for (a) and (b).

Scheme 2. Mechanisms of ICAR ATRP

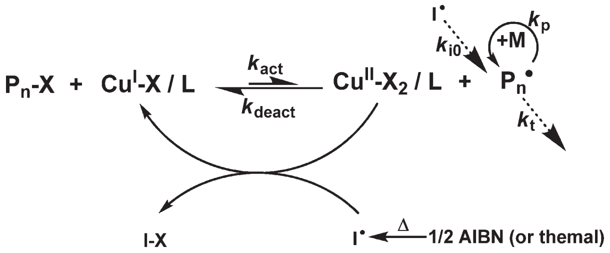

simulations, polymer chains terminated with an α-I group and an α-R group are distinguished. ICAR ATRP of St, a well-studied system, was chosen for these simulations. Since we are only concerning how many polymer chains were initiated by $I^\bullet$ and $R^\bullet$, respectively, those generated through thermal self-initiation of St were not considered in our simulations (especially at relatively low temperature).

Figure 8 shows how AIBN concentration affects the kinetic behavior. As $[R^\bullet]$ is determined by the rate of AIBN decomposition, the rates increase with $[AIBN]_0$. The overall DP (all polymer chains) deviates more from the theoretical value at higher $[AIBN]_0$ and MWD becomes broader. Simulation provides detailed information on the fraction of all types of chains. [T] is still defined as the concentration of terminated chains, including those forming between two polymeric radicals, between one polymeric radical and one initiator radical ($I^\bullet$ or $R^\bullet$). The terminated species generated between two $R^\bullet$ radicals and between one $R^\bullet$ radical and one $I^\bullet$ radical are also included in this population because they possess original α-CEF. This becomes even more important when R-X is macroinitiator. However, the termination between two $I^\bullet$ radicals was excluded in the population of terminated chains because it only gives small molecules. [D] is defined as the concentration of all types of dead chains, including nonextendable chains and those extendable chains possessing an α-I group. Thus, the new definitions for DCF and CEF can be expressed by eqs 18 and 19. The concentration of all chains ([all chains]) is used in eqs 18 and 19, rather than only initial ones originating from $[R\text{-}X]_0$. In a real system, the fraction of living chains present in the final product is more important than their total number. Detailed formulas for calculating [T], [D], [P-X], and [all chains] are provided in the Supporting Information.

$$\mathrm{DCF} = \frac{[\mathrm{D}]}{[\text{all chains}]} = \frac{[\mathrm{T}] + [\mathrm{I-P-X}]}{[\text{all chains}]} \qquad (18)$$

$$\mathrm{CEF} = 1 - \mathrm{DCF} = 1 - \frac{[\mathrm{T}] + [\mathrm{I-P-X}]}{[\text{all chains}]} \qquad (19)$$

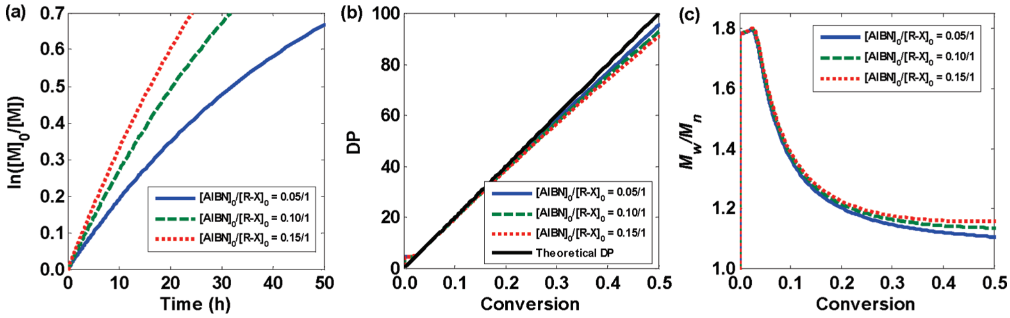

Figure 8. Results of kinetic modeling for ICAR ATRP of St. (a) Kinetic plot. (b) DP vs conversion plot. (c) M_w/M_n vs conversion plot. Conditions: 60 °C, $[St]_0/[EtBriB]_0/[CuBr_2]_0/[TPMA]_0/[AIBN]_0$ = 200/1/0.01/0.01/x (x = 0.05, 0.10, 0.15), St/acetonitrile = 2/1 (v/v) (EtBriB = ethyl 2-bromoisobutyrate; TPMA = tris[(2-pyridyl)methyl]amine; R-X = EtBriB).

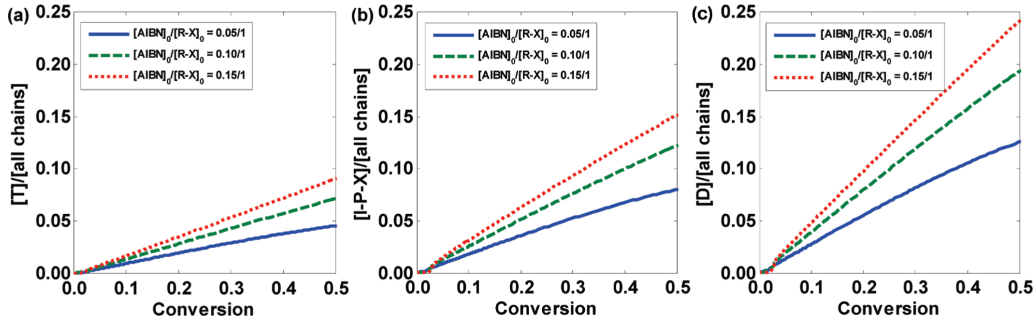

Figure 9. Plots of DCF in ICAR ATRP: (a) fraction of terminated chains; (b) fraction of α-I group-terminated extendable chains; (c) fraction of all dead chains. Conditions: 60 °C, $[St]_0/[EtBriB]_0/[CuBr_2]_0/[TPMA]_0/[AIBN]_0$ = 200/1/0.01/0.01/x (x = 0.05, 0.10, 0.15), St/acetonitrile = 2/1 (v/v) (R-X = EtBriB).

In ICAR and RAFT systems, the number of extendable chains does not change, since lost R-X and R-P-X chains are replenished by I-X and I-P-X chains. Figure 9a,b shows the fractions of terminated chains and α-I group-terminated extendable chains; both of them increase with $[AIBN]_0$, meaning that faster polymerization in ICAR systems leads to more termination and larger loss of the α-R end group. Therefore, the increase of $[AIBN]_0$ increases all types of dead chains (all chains except R-X and R-P-X ones), as illustrated in Figure 9c. Thus, although formally concentration of extendable chains does not change, with 15% AIBN under our simulated conditions, there are already 9% of terminated chains at 50% conversion, and there are only 76% of chains with dual CEF left!

The difference of CEF between CRP with and without radical initiator can be compared using two representative systems: ICAR ATRP and normal ATRP. In order to provide a fair comparison, specific conditions were chosen that allow these two polymerizations to proceed at a very similar rate. Under these conditions, the differently defined CEF values are shown in Figure 10. The CEF in Figure 10a is defined as the fraction of extendable chains among initial living chains. For normal ATRP the concentration of extendable chains decreases due to unavoidable termination reactions and leading to the accumulation of persistent radicals (CuX_2/L). However, according to the conservation of X groups and steady state in ICAR ATRP, every lost X through termination is replenished by a newly generated free radical. Thus, the number of extendable chains does not decrease. Figure 10b presents the fraction of dually functionalized chains among initial living chains. The curve for normal ATRP is similar to the one in Figure 10a for every P-X chain in normal ATRP is terminated with α-R group. Although concentration of extendable chains in ICAR ATRP is constant, the replacement of some R-P-X and R-X by I-X and I-P-X causes that the corresponding curve is lower than that in Figure 10a. These two systems should lose the same amount of living chains through termination due to their similar polymerization rate. However, the termination in ICAR ATRP also involves $I\text{-}P^{\bullet}$ species while the termination in normal ATRP only leads to the decrease of [R-P-X]. Thus, the ICAR ATRP curve in Figure 10b is still higher than the one for normal ATRP. Figure 10c illustrates the fraction of extendable chains among all chains present. In a normal ATRP, [all chains] decreases through bimolecular combination, and the curve is higher than the corresponding one in Figure 10a. However, in an ICAR system, new chains are gained from the radical initiators, and the increase of [all chains] is faster than its decrease caused by combination. Although the number of extendable chains is kept constant, the increase of [all chains] decreases their fraction in final product. The final definition of CEF which is shown in Figure 10d is the fraction of dually functionalized extendable chains among all chains. The decrease of dual-CEF in ICAR system is faster than that in normal ATRP because of newly generated chains.

■ CONCLUSION

In the first part of the paper, some general rules valid for all CRPs that correlate preserved CEF with polymerization rate were presented. In order to synthesize a polymer with higher

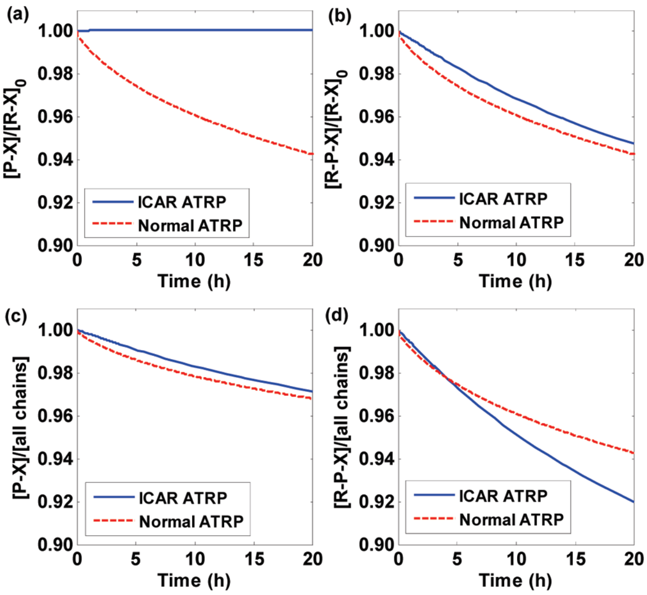

Figure 10. Comparison of CEFs in ICAR ATRP and normal ATRP according to different CEF definitions: (a) fraction of extendable chains among initial living chains; (b) fraction of dually functionalized chains among initial living chains; (c) fraction of extendable chains among all chains; (d) fraction of dually functionalized chains among all chains. Conditions: ICAR ATRP, 60 °C, $[\mathrm{St}]_0/[\mathrm{EtBriB}]_0/[\mathrm{CuBr_2}]_0/[\mathrm{TPMA}]_0/[\mathrm{AIBN}]_0$ = 200/1/0.01/0.01/0.05, St/acetonitrile = 2/1 (v/v); normal ATRP, 60 °C, $[\mathrm{St}]_0/[\mathrm{EtBriB}]_0/[\mathrm{CuBr}]_0/[\mathrm{CuBr_2}]_0/[\mathrm{PMDETA}]_0$ = 200/1/0.945/0.055/1, St/acetonitrile = 2/1 (v/v) (PMDETA: *N,N,N′,N″,N″*-pentamethyldiethylenetriamine; R-X = EtBriB).

CEF at the same rate, lower DP$_\mathrm{T}$, lower conversion, higher initial monomer concentration, and bulk conditions should be used. For the synthesis of a polymer with a certain DP during the specific time frame, it is beneficial to target higher DP$_\mathrm{T}$ and stop the reaction at lower conversion rather than the opposite way (lower DP$_\mathrm{T}$ and higher conversion). The minimal polymerization time for preserved CEF strongly depends on monomer structure. Monomers with lower $k_t/(k_p)^2$ values allow a faster polymerization with the same CEF. Also, CLDT, higher temperature and higher pressure are beneficial because they decrease $k_t/(k_p)^2$ values.

In the second part, two definitions for CEF were introduced. The first one defines total number of extandable chains, and the second one defines chains with dual funcationality, which is important for block copolymerization, surface grafting, and telechelics. The distinction is needed for DT systems such as RAFT but also for ICAR ATRP. In ICAR ATRP, although the number of extendable chains does not decrease, the generation of new chains from radical initiators results in a larger loss of dual CEF in comparison with normal ATRP at a comparable rate.

■ ASSOCIATED CONTENT

Ⓢ **Supporting Information.** CLDT rate coefficient for bulk polymerization of MMA at 80 °C; kinetic models, rate constants, and kinetic plots for the simulations of ICAR ATRP and normal ATRP of St at 60 °C; formulas for calculating [T], [D], [P-X], and [all chains] in ICAR ATRP and normal ATRP. This material is available free of charge via the Internet at http://pubs.acs.org.

■ AUTHOR INFORMATION

Corresponding Author

*E-mail: km3b@andrew.cmu.edu.

■ ACKNOWLEDGMENT

The authors thank the National Science Foundation (CHE-10-26060) and the members of the CRP Consortium at Carnegie Mellon University for their financial support. The authors also thank Yu Wang, Dr. Yungwan Kwak, and Dr. Matthew Tonge for their useful comments.

■ REFERENCES

(1) Szwarc, M. *Nature* **1956**, *178* (4543), 1168–1169.
(2) Szwarc, M.; Levy, M.; Milkovich, R. *J. Am. Chem. Soc.* **1956**, *78* (11), 2656–2657.
(3) Baskaran, D.; Müller, A. H. E. *Prog. Polym. Sci.* **2007**, *32* (2), 173–219.
(4) Bielawski, C. W.; Grubbs, R. H. *Prog. Polym. Sci.* **2007**, *32* (1), 1–29.
(5) Braunecker, W. A.; Matyjaszewski, K. *Prog. Polym. Sci.* **2007**, *32* (1), 93–146.
(6) Domski, G. J.; Rose, J. M.; Coates, G. W.; Bolig, A. D.; Brookhart, M. *Prog. Polym. Sci.* **2007**, *32* (1), 30–92.
(7) Goethals, E. J.; Du Prez, F. *Prog. Polym. Sci.* **2007**, *32* (2), 220–246.
(8) Penczek, S.; Cypryk, M.; Duda, A.; Kubisa, P.; Slomkowski, S. *Prog. Polym. Sci.* **2007**, *32* (2), 247–282.
(9) Yokozawa, T.; Yokoyama, A. *Prog. Polym. Sci.* **2007**, *32* (1), 147–172.
(10) Hadjichristidis, N.; Iatrou, H.; Pitsikalis, M.; Mays, J. *Prog. Polym. Sci.* **2006**, *31* (12), 1068–1132.
(11) Matyjaszewski, K.; Gnanou, Y.; Leibler, L. *Macromolecular Engineering: From Precise Macromolecular Synthesis to Macroscopic Materials Properties and Applications*; Wiley-VCH: Weinheim, 2007.
(12) Müller, A. H. E.; Matyjaszewski, K. *Controlled and Living Polymerizations: From Mechanisms to Applications*; Wiley-VCH: Weinheim, 2009.
(13) Hawker, C. J.; Bosman, A. W.; Harth, E. *Chem. Rev.* **2001**, *101* (12), 3661–3688.
(14) Wayland, B. B.; Poszmik, G.; Mukerjee, S. L.; Fryd, M. *J. Am. Chem. Soc.* **1994**, *116* (17), 7943–7944.
(15) Wang, J. S.; Matyjaszewski, K. *J. Am. Chem. Soc.* **1995**, *117* (20), 5614–5615.
(16) Matyjaszewski, K.; Xia, J. H. *Chem. Rev.* **2001**, *101* (9), 2921–2990.
(17) Kato, M.; Kamigaito, M.; Sawamoto, M.; Higashimura, T. *Macromolecules* **1995**, *28* (5), 1721–1723.
(18) Kamigaito, M.; Ando, T.; Sawamoto, M. *Chem. Rev.* **2001**, *101* (12), 3689–3745.
(19) Tsarevsky, N. V.; Matyjaszewski, K. *Chem. Rev.* **2007**, *107* (6), 2270–2299.
(20) Matyjaszewski, K.; Tsarevsky, N. V. *Nature Chem.* **2009**, *1* (4), 276–288.
(21) di Lena, F.; Matyjaszewski, K. *Prog. Polym. Sci.* **2010**, *35* (8), 959–1021.
(22) Chiefari, J.; Chong, Y. K.; Ercole, F.; Krstina, J.; Jeffery, J.; Le, T. P. T.; Mayadunne, R. T. A.; Meijs, G. F.; Moad, C. L.; Moad, G.; Rizzardo, E.; Thang, S. H. *Macromolecules* **1998**, *31* (16), 5559–5562.
(23) Moad, G.; Rizzardo, E.; Thang, S. H. *Aust. J. Chem.* **2005**, *58* (6), 379–410.
(24) Yamago, S. *Chem. Rev.* **2009**, *109* (11), 5051–5068.
(25) Gaynor, S. G.; Wang, J. S.; Matyjaszewski, K. *Macromolecules* **1995**, *28* (24), 8051–8056.

(26) Matyjaszewski, K.; Gaynor, S.; Wang, J. S. *Macromolecules* **1995**, *28* (6), 2093–2095.

(27) Greszta, D.; Mardare, D.; Matyjaszewski, K. *Macromolecules* **1994**, *27* (3), 638–644.

(28) Matyjaszewski, K. *J. Phys. Org. Chem.* **1995**, *8* (4), 197–207.

(29) Matyjaszewski, K.; Gaynor, S.; Greszta, D.; Mardare, D.; Shigemoto, T. *J. Phys. Org. Chem.* **1995**, *8* (4), 306–315.

(30) Goto, A.; Fukuda, T. *Prog. Polym. Sci.* **2004**, *29* (4), 329–385.

(31) Xia, J. H.; Matyjaszewski, K. *Macromolecules* **1997**, *30* (25), 7692–7696.

(32) Gromada, J.; Matyjaszewski, K. *Macromolecules* **2001**, *34* (22), 7664–7671.

(33) Jakubowski, W.; Matyjaszewski, K. *Macromolecules* **2005**, *38* (10), 4139–4146.

(34) Jakubowski, W.; Matyjaszewski, K. *Angew. Chem., Int. Ed.* **2006**, *45* (27), 4482–4486.

(35) Matyjaszewski, K.; Jakubowski, W.; Min, K.; Tang, W.; Huang, J. Y.; Braunecker, W. A.; Tsarevsky, N. V. *Proc. Natl. Acad. Sci. U.S.A.* **2006**, *103* (42), 15309–15314.

(36) Fischer, H. *Chem. Rev.* **2001**, *101* (12), 3581–3610.

(37) Tang, W.; Tsarevsky, N. V.; Matyjaszewski, K. *J. Am. Chem. Soc.* **2006**, *128* (5), 1598–1604.

(38) Tang, W.; Fukuda, T.; Matyjaszewski, K. *Macromolecules* **2006**, *39* (13), 4332–4337.

(39) Percec, V.; Guliashvili, T.; Ladislaw, J. S.; Wistrand, A.; Stjerndahl, A.; Sienkowska, M. J.; Monteiro, M. J.; Sahoo, S. *J. Am. Chem. Soc.* **2006**, *128* (43), 14156–14165.

(40) Machado, M.; Faucher, S.; Zhu, S. P. *J. Polym. Sci., Part A: Polym. Chem.* **2010**, *48* (11), 2294–2301.

(41) Matyjaszewski, K. *Prog. Polym. Sci.* **2005**, *30* (8−9), 858–875.

(42) Greszta, D.; Matyjaszewski, K. *Macromolecules* **1996**, *29* (24), 7661–7670.

(43) Buback, M.; Busch, M.; Lammel, R. A. *Macromol. Theory Simul.* **1996**, *5* (5), 845–861.

(44) Buback, M.; Busch, M.; Kowollik, C. *Macromol. Theory Simul.* **2000**, *9* (8), 442–452.

(45) Barner-Kowollik, C.; Quinn, J. F.; Morsley, D. R.; Davis, T. P. *J. Polym. Sci., Part A: Polym. Chem.* **2001**, *39* (9), 1353–1365.

(46) Vana, P.; Davis, T. P.; Barner-Kowollik, C. *Macromol. Theory Simul.* **2002**, *11* (8), 823–835.

(47) Tang, W.; Matyjaszewski, K. *Macromol. Theory Simul.* **2008**, *17* (7−8), 359–375.

(48) Wulkow, M. *Macromol. Theory Simul.* **1996**, *5* (3), 393–416.

(49) Buback, M.; Kurz, C. H.; Schmaltz, C. *Macromol. Chem. Phys.* **1998**, *199* (8), 1721–1727.

(50) Beuermann, S.; Buback, M.; Davis, T. P.; Garcia, N.; Gilbert, R. G.; Hutchinson, R. A.; Kajiwara, A.; Kamachi, M.; Lacik, I.; Russell, G. T. *Macromol. Chem. Phys.* **2003**, *204* (10), 1338–1350.

(51) Buback, M.; Gilbert, R. G.; Hutchinson, R. A.; Klumperman, B.; Kuchta, F. D.; Manders, B. G.; Odriscoll, K. F.; Russell, G. T.; Schweer, J. *Macromol. Chem. Phys.* **1995**, *196* (10), 3267–3280.

(52) Buback, M.; Egorov, M.; Gilbert, R. G.; Kaminsky, V.; Olaj, O. F.; Russell, G. T.; Vana, P.; Zifferer, G. *Macromol. Chem. Phys.* **2002**, *203* (18), 2570–2582.

(53) Barner-Kowollik, C.; Buback, M.; Egorov, M.; Fukuda, T.; Goto, A.; Olaj, O. F.; Russell, G. T.; Vana, P.; Yamada, B.; Zetterlund, P. B. *Prog. Polym. Sci.* **2005**, *30* (6), 605–643.

(54) Johnston-Hall, G.; Stenzel, M. H.; Davis, T. P.; Barner-Kowollik, C.; Monteiro, M. J. *Macromolecules* **2007**, *40* (8), 2730–2736.

(55) Theis, A.; Davis, T. P.; Stenzel, M. H.; Barner-Kowollik, C. *Macromolecules* **2005**, *38* (24), 10323–10327.

(56) Beuermann, S.; Buback, M. *Prog. Polym. Sci.* **2002**, *27* (2), 191–254.

(57) Kwiatkowski, P.; Jurczak, J.; Pietrasik, J.; Jakubowski, W.; Mueller, L.; Matyjaszewski, K. *Macromolecules* **2008**, *41* (4), 1067–1069.

(58) Rzayev, J.; Penelle, J. *Macromolecules* **2002**, *35* (5), 1489–1490.

(59) Rzayev, J.; Penelle, J. *Angew. Chem., Int. Ed.* **2004**, *43* (13), 1691–1694.

(60) Monteiro, M. J.; Bussels, R.; Beuermann, S.; Buback, M. *Aust. J. Chem.* **2002**, *55* (6−7), 433–437.

(61) Arita, T.; Buback, M.; Janssen, O.; Vana, P. *Macromol. Rapid Commun.* **2004**, *25* (15), 1376–1381.